Geobios 52 (2019) 67–83

Available online at
ScienceDirect
www.sciencedirect.com

Elsevier Masson France
EM|consulte
www.em-consulte.com

Original article

The Madenli (Central Taurides) Upper Cretaceous platform carbonate succession: Benthic foraminiferal biostratigraphy and platform evolution☆

Cemile Solak [a,*], Kemal Taslı [a], Sacit Özer [b], Hayati Koç [a]

[a] Mersin University, Faculty of Engineering, Department of Geological Engineering, Çiftlikköy Campus, 33343 Mersin, Turkey
[b] Dokuz Eylül University, Faculty of Engineering, Department of Geological Engineering, İzmir, Turkey

ARTICLE INFO

Article history:
Received 14 December 2017
Accepted 15 November 2018
Available online 27 November 2018

Keywords:
Benthic foraminifera
Rudist
Microfacies
Carbonate platform
Paleoenvironments
Platform emersion

ABSTRACT

The Upper Cretaceous succession in the Madenli area (western Central Taurides, Southern Turkey) consists of platform carbonate rocks deposited in entirely peritidal environments, which are sensitive to sea level changes driven by global eustasy, but also strongly affected by local and regional tectonics. It includes economically important bauxite deposits. Previous works suggest different ages for bauxite formation ranging from the Albian to the Santonian. Benthic foraminiferal biostratigraphy and facies analysis of the Madenli and Doğankuzu outcrop sections allow for a more precise dating of the platform emersion periods. The footwall limestones of the bauxite deposits consist of well-bedded limestones (Unit-1), which contain a benthic foraminiferal assemblage (BFA) including mainly *Biconcava bentori* and *Pastrikella biplana*, *Chrysalidina gradata* (BFA I), assigned to the middle-upper Cenomanian. In the Madenli section, the first bauxite deposit occurs in the upper part of Unit-1 as a layer interbedded with pinkish sparitic and dolomitic beds (subunit-1a) deposited in supratidal environment. Subunit-1a is stratigraphically equivalent to the Doğankuzu and Mortaş bauxite deposits considered as karst-related, unconformity-type deposits. The hanging-wall limestones of the bauxite are represented by the massive limestones (Unit-2) starting locally with either the upper Cenomanian characterized mainly by the presence of *Pseudolituonella reicheli* or upper Campanian comprising mainly *Murciella cuvillieri* and *Moncharmontia apenninica* (BFA II). There is no field evidence of a discontinuity surface at the contact between the lower part of Unit-2, including BFA I, and the upper part of Unit-2, including BFA II. This contact is defined as a paraconformity indicating a stratigraphic gap from the Turonian to the early Campanian. The top of Unit-2 is truncated by another discontinuity surface associated with a minor bauxite deposit. The overlying Unit-3 is characterized by well-bedded, rudist-bearing limestones topped by laminated and dolomitized limestones organized in shallowing upward cycles. It is assigned to the upper Maastrichtian based on the presence of *Rhapydionina liburnica* (BFA III) and rudist assemblage. A third emersion period of the platform corresponds to the early Maastrichtian.

1. Introduction

The Upper Cretaceous succession of platform carbonates in the Seydişehir area, south of Turkey (Fig. 1), hosts economically important karst-related bauxite deposits which have mainly been subject to geochemical studies (Blumenthal and Göksu, 1949; Wippern, 1962; Martin, 1969; Atabey, 1976; Monod, 1977; Özlü, 1978; Öztürk et al., 2002), including age data on the limestones surrounding bauxite deposits. Proposed ages for the main bauxite deposit range from the Albian/Cenomanian to the Santonian.

In the absence of pelagic fauna, the Upper Cretaceous biostratigraphy of platform carbonates relies largely on relatively long ranging benthic foraminifera, which have a low stratigraphic resolution (e.g., Velić, 2007; Chiocchini et al., 2008). The existing data (Fig. 2) show that the main causes of controversies on the age of the bauxite deposits are due to the scarcity of age-diagnostic taxa and differences arising from chronostratigraphic attribution of biostratigraphic data (Özlü, 1978; Öztürk et al., 2002; Karadağ et al., 2009). Previous studies have been mainly focused on the bauxite deposits in the Mortaş and Doğankuzu localities, but paleontology and sedimentology of the Madenli Upper Cretaceous

☆ Corresponding editor: Fabienne Giraud-Guillot.

* Corresponding author.
E-mail address: cemilesolak@mersin.edu.tr (C. Solak).

https://doi.org/10.1016/j.geobios.2018.11.006
0016-6995/

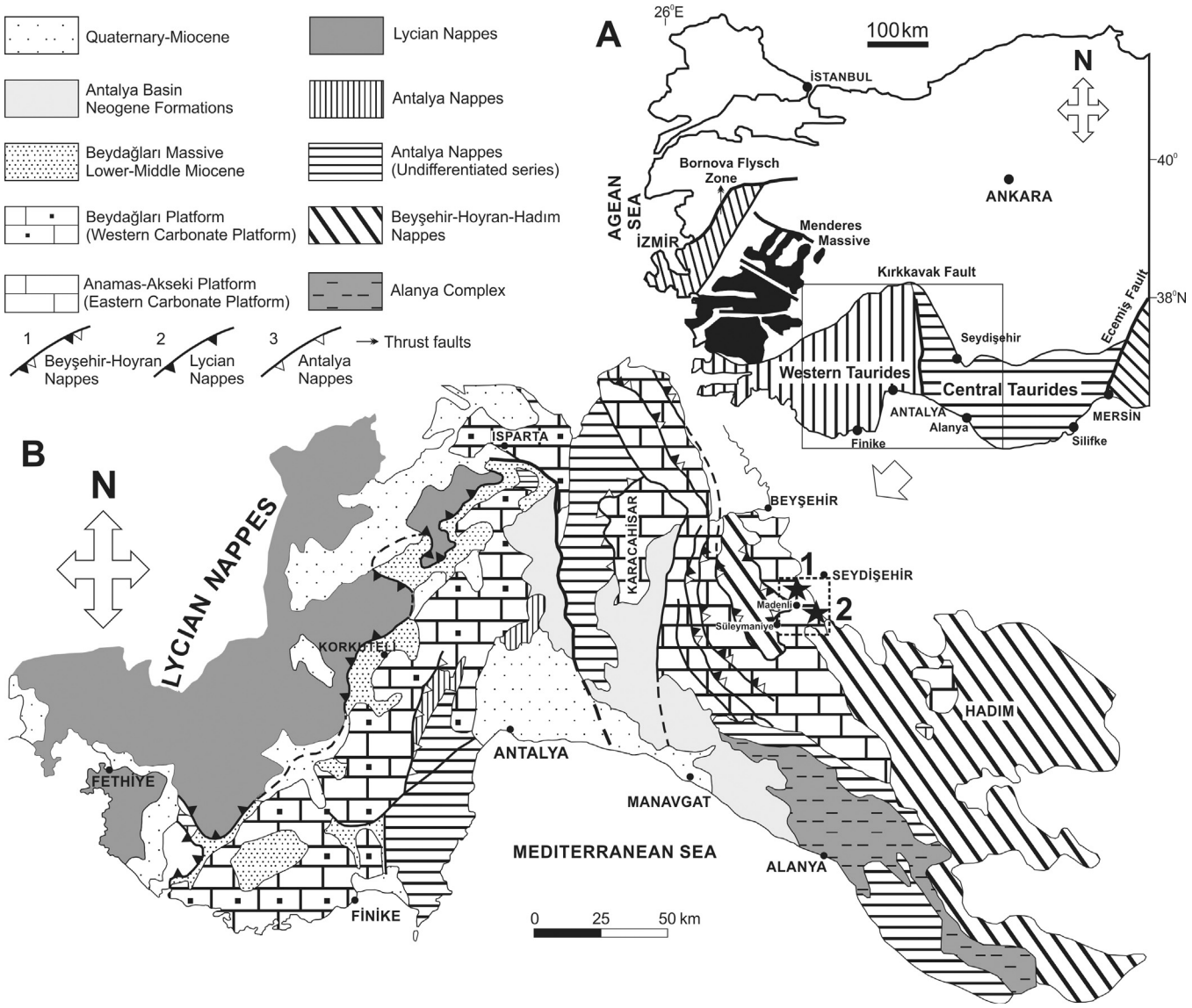

Fig. 1. A. Geographic subdivision of the Taurides (Özgül, 1984). **B**. Structural map of the Central and Western Taurides (after Poisson et al., 1984) showing the location of the measured stratigraphic sections (black asterisks): 1, Madenli section; 2, Doğankuzu section (see Fig. 3 for a detailed map of the Madenli area).

succession have not been studied until now in detail. Therefore, the platform evolution remains not well understood.

The present study aims:

- to provide higher resolution ages of the succession by using benthic foraminiferal biostratigraphy integrated with rudist biostratigraphy;
- to explain the platform evolution by interpreting depositional environments based on microfacies analysis and to define stratigraphic gaps during the Late Cretaceous in the western Central Taurides.

2. Geological setting

The Central Taurides is bounded by two major strike slip faults: the Kırkkavak fault to the west and the Ecemiş fault to the east (Özgül, 1984) (Fig. 1). The Madenli (Seydişehir) area is located at the western part of the Central Taurides. The regional stratigraphic succession starts with the Lower-Middle Cambrian recrystallized dolostones and limestones (Çaltepe Fm.) and the Upper Cambrian-Lower Ordovician phyllites interbedded with metasandstones (Seydişehir Fm.) (Dean and Monod, 1970). The unconformably overlying Triassic units consist of clastic rocks and limestones. The Middle Jurassic to Upper Cretaceous is represented by purely platform carbonate rocks, which host bauxite deposits in the Upper Cretaceous. These Paleozoic and Mesozoic units together with the unconformably overlying Paleocene-Eocene sediments form a regional parautochthonous unit called the "Anamas-Akseki unit" (Dumont and Kerey, 1975), "Geyikdağ unit" (Özgül, 1976), or "Anamas-Akseki platform" (Poisson et al., 1984). This tectonostratigraphic unit is overlain by the Beyşehir-Hoyran-Hadım nappes (Dumont, 1976; Poisson et al., 1984) consisting mainly of Mesozoic carbonate platform, deep-sea and ophiolitic units (Andrew and Robertson, 2002). The regional geology is further detailed in Özgül (1976), Monod (1977), Özgül (1984), and Demirtaşlı (1984).

The Upper Cretaceous carbonate succession that is the focus of this study is divided into two formations: the Cenomanian Katrangediği Fm. below the bauxite deposits, and the Senonian Doğankuzu Fm. above the bauxite deposits (Karadağ et al., 2009). Its basal part is in normal-faulted contact with the Eocene units

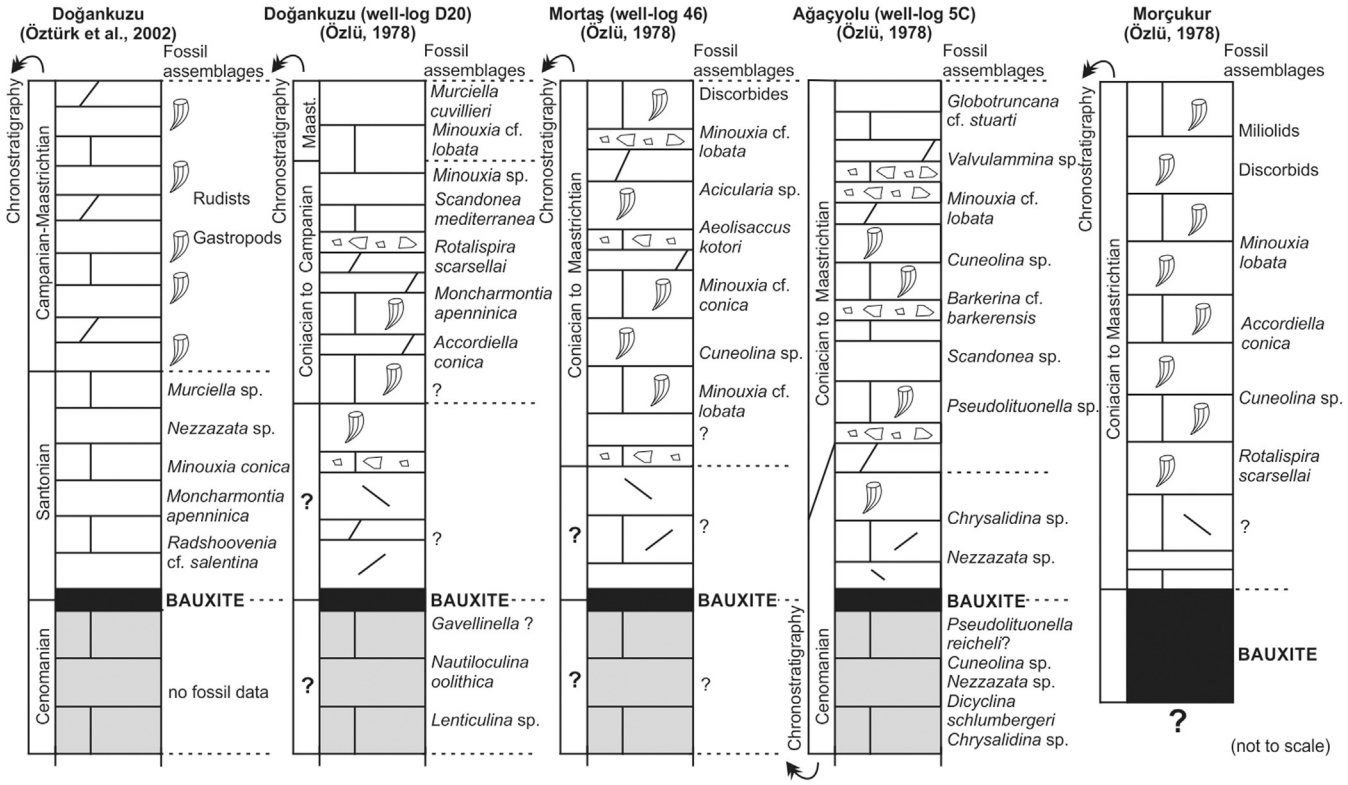

Fig. 2. Correlations between previous studies showing the Upper Cretaceous micropaleontologic data in the Madenli area.

(map of Fig. 3). It is unconformably overlain by the lower Eocene algal limestones and middle to upper Eocene nummulitid limestones, pelagic limestones and siliciclastic sediments.

3. Material and methods

The Upper Cretaceous succession studied here is exposed along the northwest and southeast of Madenli village, south of Seydişehir (Fig. 1). The Madenli-II section (37°19′46.45″N, 31°49′26.34″E; II in Fig. 3), chosen as the reference section, is located on the rural road from Madenli village to Süleymaniye village, at km 6. This is the most complete, easily accessible and relatively undisturbed succession in which vertical and lateral relationships between the lithological units are well exposed. The Doğankuzu section (37°16′27.02″N, 31°53′24.58″E; III in Fig. 3) was sampled from the nearby Doğankuzu bauxite quarry. An additional section was measured from the north of the Madenli section-II (37°19′55.96″N, 31°48′57.42″E; I in Fig. 3). Also, we made field observations to recognize changes in thickness and facies of the lithological units around the Doğankuzu and Mortaş bauxite deposits.

Samples were collected at 0.5 m intervals along the boundaries between the lithological units and at 2 m intervals in monotonous and massive levels. In total, 270 thin sections from 240 samples were analyzed for microfacies and microfossil content. Microfacies classification of limestone samples is based on the nomenclature of Dunham (1962) and Embry and Klovan (1971), and followed by a semi quantitative analysis of the components. We have followed the guidelines of previous investigations such as Flügel (2004) and Golubic et al. (2006) for the paleoenvironmental attribution of microfacies described here. The samples and thin sections (md 1 to 223 from the Madenli-II section, mda 1 to 8 from north of the Madenli-II section, and dkz 1-3a, 3b-8 from the Doğankuzu section) used for this study are housed at the Department of Geological Engineering, Mersin University, Turkey (collection C. Solak). The geologic time scale and substage duration is after Gradstein et al. (2012).

We have also used G. Bignot's micropaleontologic determinations in Özlü (1978) who presented many well-logs (Fig. 2) across the footwall and hanging-wall limestones of bauxite deposits. These logs are chronostratigraphically reinterpreted taking into account current knowledge of the stratigraphic ranges of some stratigraphically important benthic foraminiferal taxa such as *Murciella* and *Accordiella* (Frijia et al., 2015; Fleury, 2016).

Rudists are mostly embedded within the limestones so it was impossible to collect matrix-free specimens. However, field photos and polished sections of some rudist-bearing limestone samples were used for their description.

4. Results

4.1. Lithostratigraphy and facies

The Madenli Upper Cretaceous succession is *ca.* 240 m in thickness. It is herein subdivided into three informal lithological units based on bedding features, sedimentary structures and macrofossils. The stratigraphic section details are given below. The six microfacies associations (MFA) have been distinguished by sedimentological analysis of the studied sections and summarized in Table 1. Fossil content (see Appendix A) of the lithological units are presented in Fig. 4 and detailed in Section 4.2.

4.1.1. Unit-1 (middle-upper Cenomanian)

Unit-1 is 75–80 m in thickness and consists of mainly grey-coloured, thick to very thick (0.5–2 m) and well-bedded limestones. In its upper part, subunit-1a is composed of 5–10 m thick, pinkish sparitic and yellowish dolomitic beds with a bauxite layer (Fig. 5(A, B)). The lateral extent of the bauxite layer, up to 12 cm in thickness, cannot be followed because of debris cover. Unit-1 is

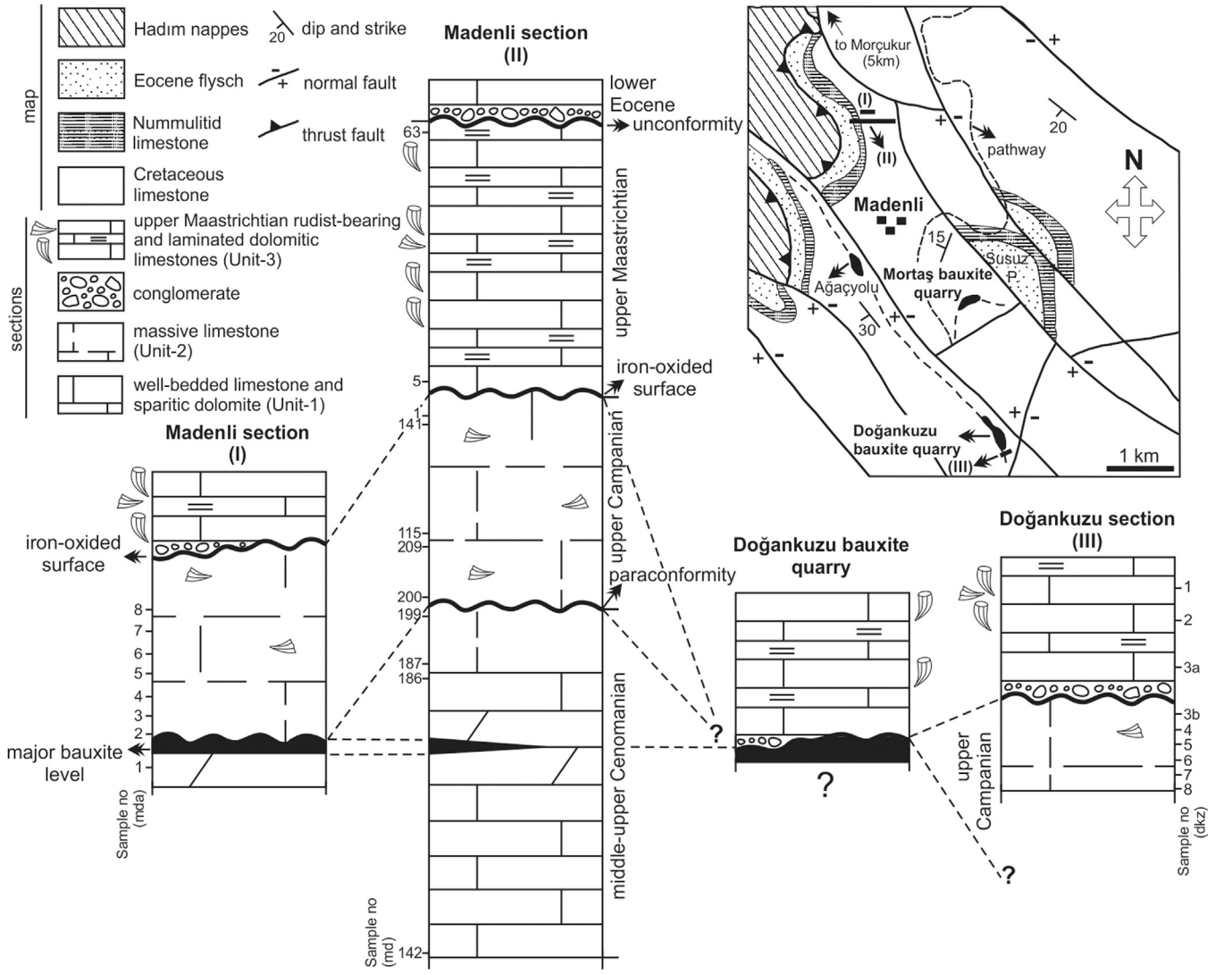

Fig. 3. Geological map (after Özlü, 1978) showing the locations of the measured stratigraphic sections and bauxite deposits in the Madenli area, and north-south correlations of the Upper Cretaceous carbonate sections studied in the Madenli area.

completely devoid of macrofossils, except for rare bivalve shell fragments.

Unit-1 is characterized by the predominance of intraclastic-benthic foraminiferal packstone/grainstone, laminated peloidal packstone/grainstone (MFA-1) intercalated with mudstone with fenestrae/birdeyes, ostracod wackestone (MFA-2), and rarely benthic foraminiferal-microbial wackestone (MFA-3) (Fig. 6). Low diversity, abundance of intraclast/peloids, presence of fenestrae/birdeyes, lamination and local abundance of ostracods suggest restricted inner platform environments. Unit-1 deposited in dominantly shallow subtidal environment. Bauxite deposits and dolomitic intercalations (Subunit-1a) probably resulted from exposure of the platform to partly subaerial and supratidal environments in addition to other factors such as climatic conditions and source material.

4.1.2. Unit-2 (upper Cenomanian and upper Campanian)

Unit-2 is characterized by grey-beige coloured, massive limestones (2–3 m; Fig. 5(C)); the upper part of Unit-2 includes mm-scale rudist fragments. In contrast with lithological continuity and uniformity through massive limestone unit (Unit-2), there is a major change in benthic foraminiferal assemblage at 25 m from the base of the Unit-2, between samples md 199 and md 200 (see Section 4.2.). This change follows the change to muddy-rich microfacies (MFA-3 and 4; Fig. 6) with mm-sized rudist fragments. Thus, the contact between the lower and upper parts of Unit-2 is defined as a paraconformity that indicates a major stratigraphic gap spanning the interval from the Turonian to the lower Campanian. Due to this paraconformity, the uppermost part of Unit-1 and lower part of Unit-2 are missing in some localities where the bauxite deposit is immediately overlain by the upper part of Unit-2. Upper boundary of Unit-2 is truncated by a marked erosional surface, characterized by the presence of rhizolites and iron-oxided surfaces (Fig. 5(D)), which corresponds to the minor bauxite level of Öztürk et al. (2002).

Microfacies of the lower part of Unit-2 are identical to those of Unit-1 and suggest restricted platform settings. The upper part of Unit-2 comprises alternations of benthic foraminiferal-microbial wackestone (MFA-3) with bioclastic (mostly rudist fragments) wackestone/packstone/floatstone (MFA-4). MFA-3 is the most widespread microfacies in the succession, representing about 38% of the samples. Low number of individuals and scarcely diversified benthic foraminifera (the most dominant are nubeculariids, discorbids, and miliolids to a lesser extent), *Decastronema*, *Thaumatoporella* and fenestrae show that restricted environments prevail (Carannante et al., 2000). Angular rudist fragments

Table 1
Microfacies associations identified in the Madenli Upper Cretaceous platform carbonate succession.

Microfacies Association (MFA)	Components (skeletal and non-skeletal)	Sedimentary structures	Environments
MFA-1. Intraclastic-benthic foraminiferal packstone/grainstone and laminated peloidal packstone/grainstone (Fig. 6(A, B))	Intraclast (va), peloid (a), imperforate benthic foraminifera (c), ostracod (r), bivalve shell (r), gastropod (r), *Thaumatoporella* (r), *Gahkumella* (r) and *Decastronema* (r)	Lamination in mm-scale (commonly resulting from changing proportions of peloid, intraclast and muddy matrix from one laminae to other), fenestrae	Restricted platform environments including peritidal and shallow pond settings
MFA-2. Mudstone with fenestrae/birdeyes, ostracod wackestone (Fig. 6(C))	Ostracod (la), discorbid (r), miliolid (r) and algal-structure (r)	Fenestrae (c) (infilled by sparitic cement or geopetally internal silt-sized sediment), rarely birdeyes, locally lamination	Restricted shallow environments (supratidal-intertidal, shallow pond settings)
MFA-3. Benthic foraminiferal-microbial wackestone (Fig. 6(D, E))	Benthic foraminifera (a) (mainly nubeculariid, discorbid, miliolid and other imperforate forms), *D. kotori-D. barattoloi* (c), *Thaumatoporella* (c). *Gahkumella* (r), ostracod (r), gastropod (r), dasycladacean algae (r), rudist fragment (r), bivalve shell (r)	Fenestrae, lamination (alternation of mm- or cm-thick laminae of differences in the abundance of nubeculariid, other foraminifera and rarely mud, peloids)	Restricted shallow environments (peritidal)
MFA-4. Bioclastic (rudist-bearing) wackestone/packstone/floatstone (Fig. 6(F))	Bioclast (a) (poorly-sorted rudist fragments), imperforate benthic foraminifera (c)	Bioturbation, recrystallization (dolomitization), fenestrae	Shallow subtidal/subtidal with storm/wave influence
MFA-5. Wackestone with *Decastronema* (Fig. 6(G))	*Decastronema* (a), *Thaumatoporella* (c), benthic foraminifera (c) (mainly nubeculariid, miliolid and discorbid)	Lamination (originated from changing in proportions of *Decastronema* and muddy matrix.)	Peritidal environments
MFA-6. Algal wackestone (Fig. 6(H))	Dasycladalean algae (a), benthic foraminifera (mainly miliolid, discorbid) (c), nubeculariid (r), *Thaumatoporella* (r), bivalve shell (r) and gastropod (r)	Recrystallization (dolomitization)	Subtidal-Lagoon

(va): very abundant; (la): locally abundant; (a): abundant; (c): common; (r): rare.

embedded in a muddy-rich matrix alternating with benthic foraminiferal-microbial wackestone point to a relatively short transport into protected, shallow subtidal environments with low energy from nearby rudist buildups by storm/wave influence.

4.1.3. Unit-3 (upper Maastrichtian)

Unit-3 begins locally with a monomictic conglomerate (up to 1 m in thickness), which is made of pebbles derived from underlying units. It is characterized by alternation (Fig. 5(E)) of mostly 5–15 cm-thick, white laminated-dolomitic limestones and grey-coloured, 30–60 cm-thick rudist-bearing limestones (Fig. 5(F)) with collapse-breccia intercalations. Rudists in growth position are very rare; they are moderately reworked while shells are mostly toppled, and show a laterally discontinuous and patchy distributional pattern (Fig. 5(F)). Complete shells are associated with fragmented ones in rudist floatstone, and all show random orientation. Isolated individuals and groups (Fig. 5(G)) are in benthic foraminiferal deposits. Unit-3 is 75 m in thickness; it includes also irregular depositional cycles (Fig. 5(H)) varying from 10 to 80 cm in thickness, indicating a shallowing upward trend witnessed by the occurrence of upwardly thinning of shell fragments, lamination and dolomitization at top of the cycles.

This unit corresponds to a well-bedded rudist-rich bioclastic limestone, which is regionally extensive and a key stratigraphic interval, considered as Campanian or Maastrichtian in age (Öztürk et al., 2002). Field observations around the Doğankuzu and Mortaş bauxite deposits showed that the main bauxite deposit is partly overlain by Unit-3 (Fig. 3).

Unit-3 is dominated by mainly benthic foraminiferal-microbial wackestone (MFA-3) and bioclastic (rudist-bearing) wackestone/packstone/floatstone (MFA-4). Subordinate microfacies composed of mudstone with fenestrae (MFA-2), wackestone with *Decastronema* (MFA-5), and algal wackestone (MFA-6) infrequently accompany this association (Fig. 6). Shallowing depositional cycles, frequently characterized by rudist floatstone, benthic foraminiferal-microbial wackestone and fenestral mudstone, mostly correspond to subtidal to intertidal/supratidal cycles (Drobne et al., 1988; Ruberti, 1997; Carannante et al., 1998; Caffau et al., 1998). Wackestone with *Decastronema* and algal wackestone microfacies occur only at the uppermost part of Unit-3. Bioturbations on complete and fragmented rudists and abundant fragments embedded into the benthic foraminiferal wackestone, partly covered by microbial mud, suggest that the rudists inhabited a lagoonal environment (Carannante et al., 2000).

4.2. Biostratigraphy and chronostratigraphic interpretation

Three benthic foraminiferal assemblage (BFA) zones can be distinguished in the Upper Cretaceous succession of the Madenli area (Fig. 4). We preferred to use the term "assemblage" for each biozone due to the scarcity of stratigraphically important benthic foraminiferal taxa. Chronostratigraphic attributes of the biozones are based on the Mediterranean ranges of some important benthic foraminifera given in Fig. 7.

4.2.1. BFA I (middle-upper Cenomanian)

This biozone corresponds to Unit-1 and lower part of Unit-2. Miliolids and nezzazatids (Fig. 8(B, C, D)) dominate through this biozone. In order of abundance and frequency, *Spiroloculina cretacea* (Fig. 8(I, J)), *Cuneolina pavonia* (Fig. 8(R–T)), *Pseudonummoloculina heimi* (Fig. 8(M, N)), *Chrysalidina gradata* (Fig. 8(K)), *Nezzazatinella picardi* (Fig. 8(L)), and *Biconcava bentori* (Fig. 8(A)) represent the BFA I. *Glomospira* sp. (Fig. 8(E)), *Pastrikella biplana* (Fig. 8(F, G)), *Cornuspira* sp. (Fig. 8(P)), and *Pseudorhapydionina dubia* (Fig. 8(H)) are very rare and sparse. Few specimens of *Pseudolituonella reicheli* (Fig. 8(O)) occur only in the upper part of the biozone. This biozone is equivalent to the middle-upper Cenomanian Assemblage I (*Pseudorhapydionina dubia* assemblage zone) of the Kuyucak section, Central Taurides (Solak et al., 2017), the middle-upper Cenomanian *Pseudorhapydionina dubia* and *Biconcava bentori* cenozone of Bolkar Mountains (Taslı et al., 2006), the middle-upper Cenomanian *Chrysalidina gradata* superzone of Karst Dinarides (Velić, 2007), and partly to the uppermost Cenomanian *Chrysalidina gradata* and *Pseudolituonella reicheli* zone (anchored to the chronostratigraphic scale by isotope stratigraphy) of the Apennine Carbonate Platform (Frijia et al., 2015) (Fig. 9).

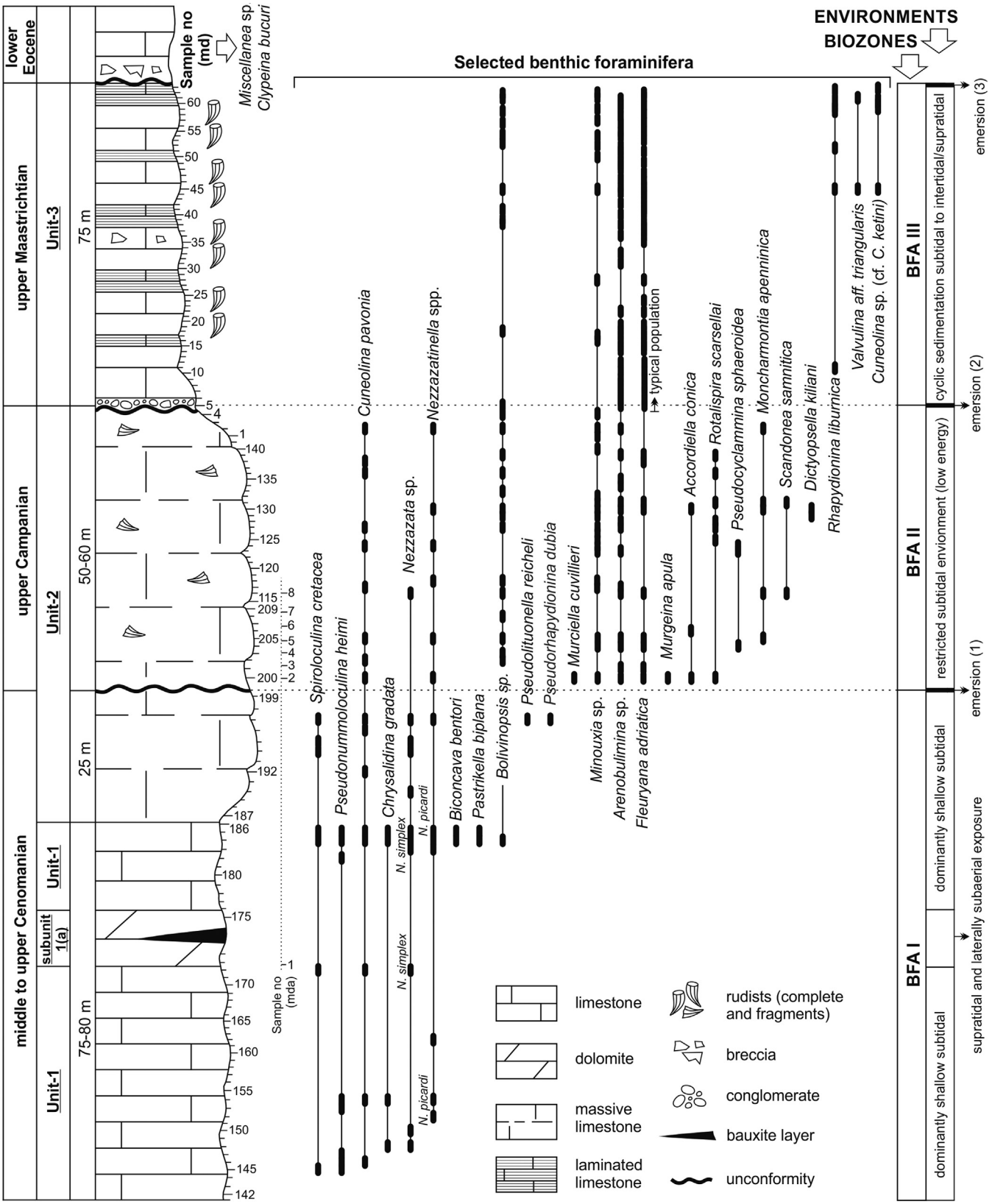

Fig. 4. Generalized stratigraphic section of the Madenli Upper Cretaceous succession showing the stratigraphic distribution of selected benthic foraminifera and depositional environments.

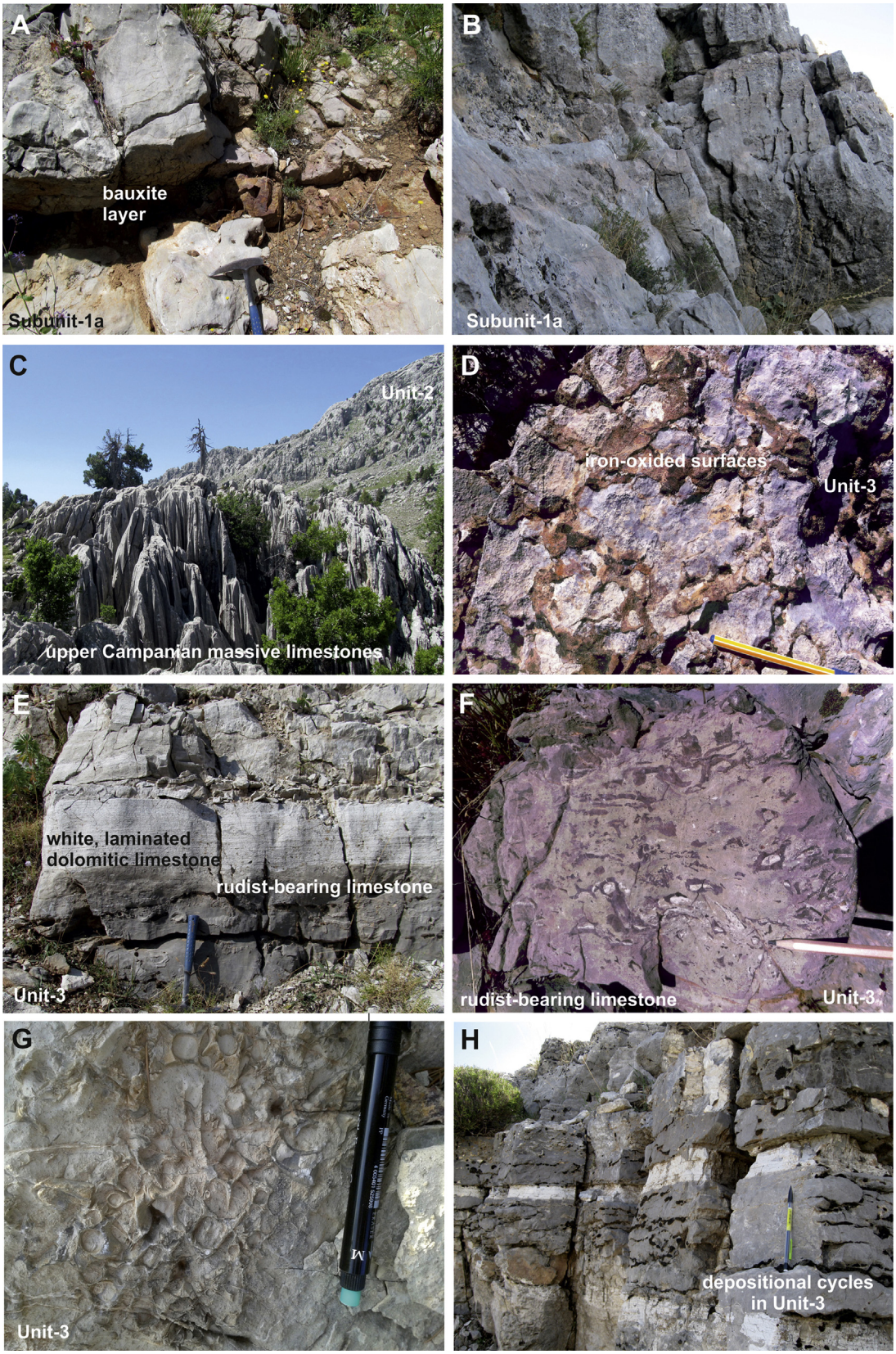

Fig. 5. Field photographs of the Upper Cretaceous platform carbonates in the Madenli and Doğankuzu measured stratigraphic sections. **A**. Middle-upper Cenomanian dolomitic-sparitic limestones with bauxite interbed (first/major bauxite; subunit-1a). **B**. Middle-upper Cenomanian pinkish sparitic-yellowish dolomitic beds (subunit-1a). **C**. Upper Campanian massive limestones (Unit-2). **D**. Iron-oxided surface. **E**. Upper Maastrichtian white, laminated-dolomitic limestones and rudist-bearing limestones (Unit-3). **F**. Upper Maastrichtian rudist-bearing limestones (Unit-3). **G**. Doğankuzu Upper Maastrichtian rudist-bearing limestones (Unit-3). **H**. Shallowing upward depositional cycles in Unit-3.

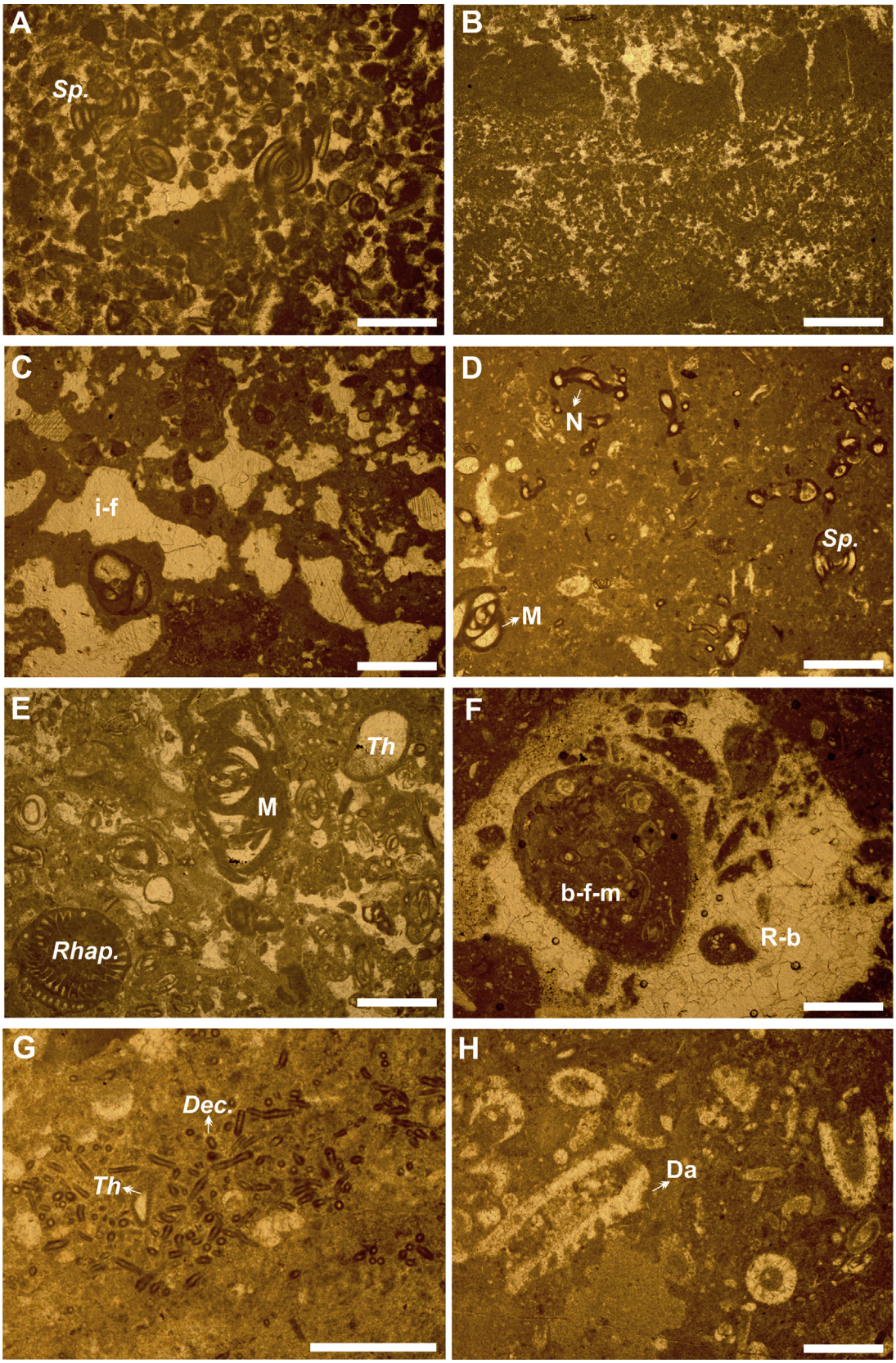

Fig. 6. Microfacies associations of the Madenli Upper Cretaceous platform carbonate succession. **A, B**. MFA-1. A. Intraclastic-benthic foraminiferal packstone/grainstone, *Sp.*: *Spiroloculina*, sample md173. B. Laminated peloidal packstone/grainstone, sample md163. **C**. MFA-2, mudstone with fenestrae, i-f: irregular fenestrae, sample md43. **D, E**. MFA-3, benthic foraminiferal-microbial wackestone, N: Nubeculariidae; M: Miliolidae; *Sp.*: *Spiroloculina*; *Rhap.*: *Rhapydionina liburnica*; *Th.*: *Thaumatoporella*, samples md44 (D), md46 (E). **F**. MFA-4, bioclastic (rudist-bearing) floatstone, b-f-m: benthic foraminiferal matrix; R-b: rudist bioeroded, sample md11. **G**. MFA-5, wackestone with *Decastronema*, *Dec.*: *Decastronema*; *Th*: *Thaumatoporella*, sample md97. **H**. MFA-6, algal wackestone, Da: Dasycladalean algae, sample md63. Scale bars: 250 μm.

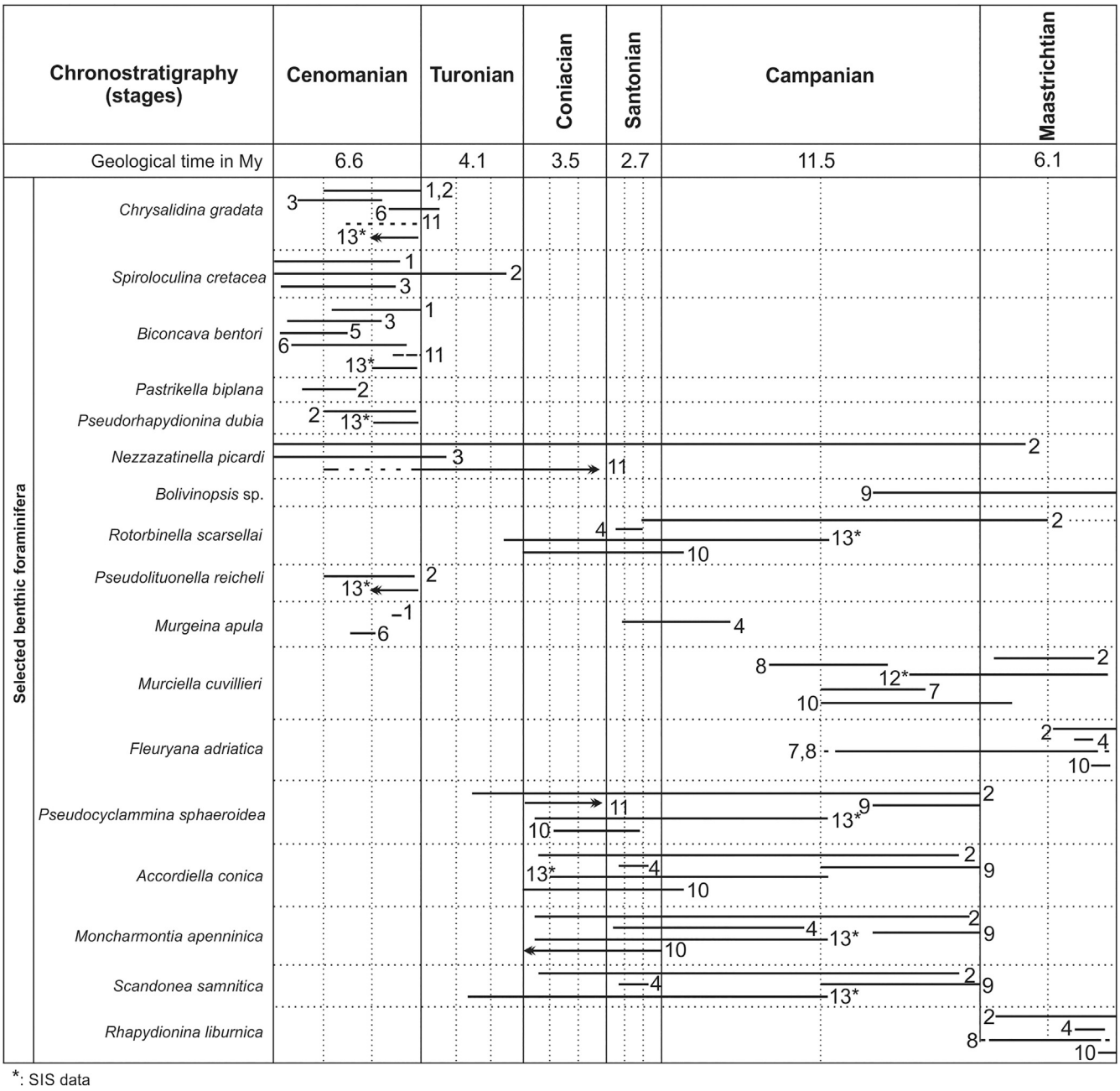

Fig. 7. Stratigraphic distribution of selected benthic foraminifera identified from the Madenli platform carbonate succession. References: 1, Velić and Vlahović (1994); 2, Velić (2007); 3, Aguilera-Franco (2003); 4, Chiocchini and Mancinelli (2001); 5, Chiocchini and Pichezz (2016); 6, Chiocchini (2008); 7, Fleury (2014); 8, Fleury (2016); 9, Solak et al. (2017); 10, Chiocchini et al. (2008); 11, Sarı et al. (2009); 12, Steuber et al. (2005); 13, Frijia et al. (2015).

4.2.2. BFA II (upper Campanian)

This biozone corresponds to the upper part of Unit-2. The most frequent, but scarce foraminifera of BFA II are *Moncharmontia apenninica* (Fig. 10(A, B)), *Fleuryana adriatica* (Fig. 10(C, D)), *Nezzazatinella* sp. (Fig. 10(E)), *Nezzazata* sp. (Fig. 10(H)), *Bolivinopsis* sp. (Fig. 10(L)), *Minouxia* sp. (Fig. 10(I)), *Arenobulimina* sp. (Fig. 10(M)), and *Cuneolina pavonia* (Fig. 10(T)). *Accordiella conica* (Fig. 10(F, G)), *Pseudocyclammina sphaeroidea* (Fig. 10(R)), *Scandonea samnitica* (Fig. 10(P, Q)), *Rotalispira scarsellai* (Fig. 10(N, O)) and poorly preserved but typical specimens of *Murciella cuvillieri* (Fig. 10(J, K)) are rarely joined to this assemblage. *Dictyopsella kiliani* (Fig. 10(S)) is represented by few specimens within only two samples. BFA II of the Madenli section corresponds to Assemblage II (*Rotalispira scarsellai* and *Murciella cuvillieri* concurrent range zone) of the Kuyucak section (Solak et al., 2017), assigned to the upper Campanian, but this biozone contains fewer benthic foraminifera in number and diversity. The chronostratigraphic constraint of the biozone is based on the fact that *Murciella* ranges no lower than the upper Campanian (Steuber et al., 2005; Velić, 2007; Fleury, 2016), and *Moncharmontia apenninica*, *Accordiella conica*, *Pseudocyclammina sphaeroidea* and *Scandonea samnitica* range no higher than the upper Campanian (Chiocchini and Mancinelli, 2001; Chiocchini et al., 2008; Fig. 7).

4.2.3. BFA III (upper Maastrichtian)

This biozone is characterized by the occurrence of *Rhapydionina liburnica* (Fig. 10(M, N)). *Fleuryana adriatica* (Fig. 11(A–G)) is very abundant and represented by larger-sized (equatorial diameter of

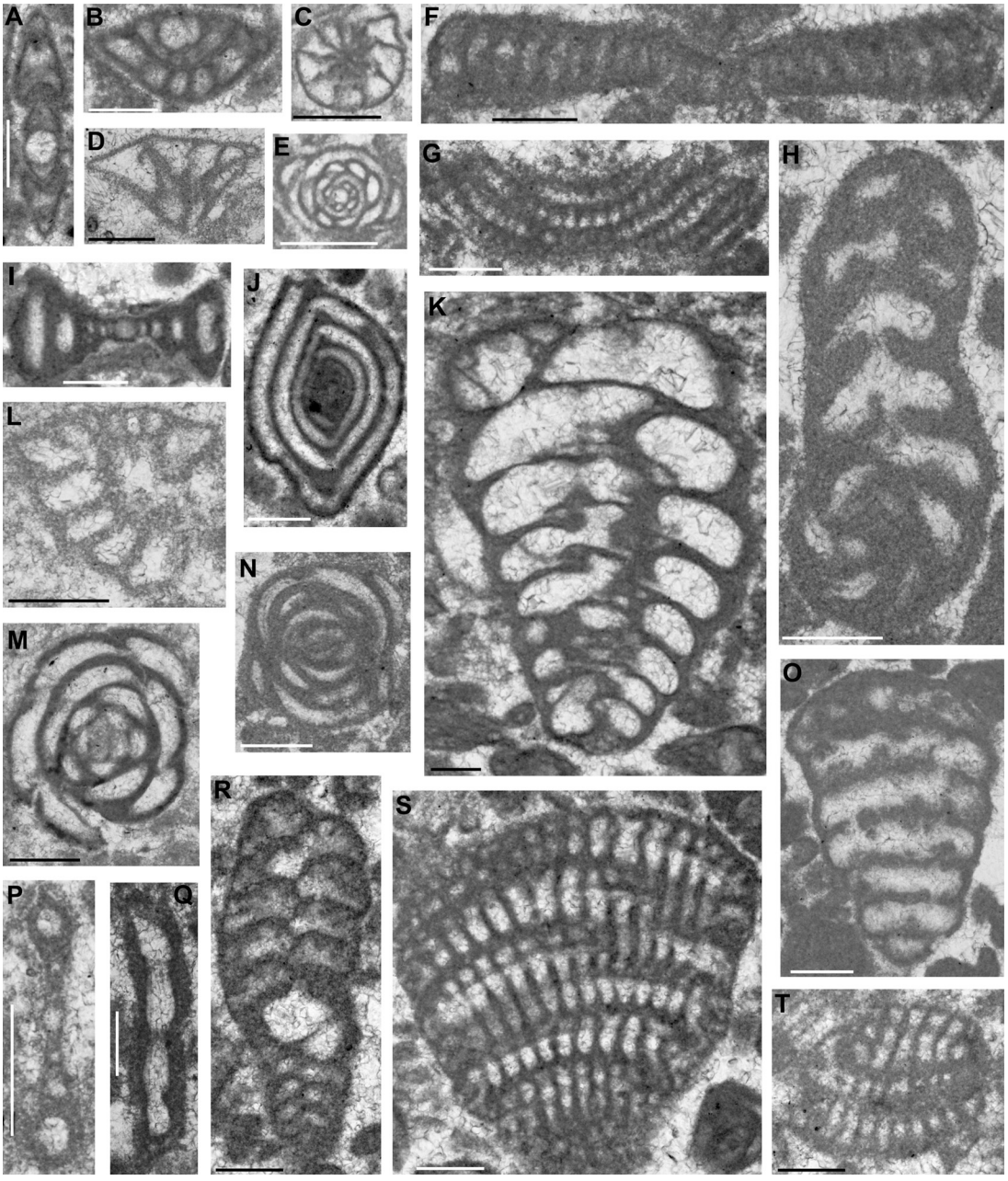

Fig. 8. Middle-upper Cenomanian benthic foraminifera (BFA I). **A**. *Biconcava bentori*, sample md184. **B, C**. *Nezzazata simplex*, samples md184 (B), md182(C). **D**. *Nezzazata gyra*, sample md184/4. **E**. *Glomospira* sp., sample md144. **F, G**. *Pastrikella biplana*, samples md184/1 (F), md184/4 (G). **H**. *Pseudorhapydionina dubia*, sample md197/2. **I, J**. *Spiroloculina cretacea*, samples md173 (I), md194 (J). **K**. *Chrysalidina gradata*, sample md154. **L**. *Nezzazatinella picardi*, sample md184/4. **M, N**. *Pseudonummoloculina heimi*, samples md145 (M), md188 (N). **O**. *Pseudolituonella reicheli*, sample md197/2. **P**. *Cornuspira sp.*, sample md184. **Q**. Nubeculariidae, sample md184. **R–T**. *Cuneolina pavonia*, samples md154 (R), md173 (S), md154 (T). Scale bars: 200 μm.

mostly 500 μm) specimens than those of the underlying biozone. *Fleuryana* sp. (Fig. 11(H, I)), which is identical to the specimen illustrated in De Castro et al. (1994: pl. 4, fig. 11), occurs in places and may belong to a new species. *Bolivinopsis* sp. (Fig. 11(J, K)), *Arenobulimina* sp. (Fig. 11(O–Q)), *Cuneolina pavonia* (Fig. 11(T)), and *Minouxia* sp. (Fig. 11(R)) continued from the underlying biozone with a rather abundant and frequent occurrence. *Valvulina* aff. *V. triangularis* (Fig. 11(S)), *Moesiloculina* sp. (Fig. 11(T)), *Elazığella* sp. (Fig. 11(U)), *Cuneolina* sp. (cf. *C. ketini*) (Fig. 11(V–X)), and nubeculariid foraminifera (Fig. 11(L)) occasionally accompany this assemblage. Dasycladalean algae (Fig. 11(Y–Z)) become abundant in the upper part of the biozone. This biozone corresponds to the upper Maastrichtian Assemblage IIIb (*Rhapy*-Rhapydionina liburnica and *Fleuryana adriatica* concurrent range subzone) of Solak et al. (2017) from Central Taurides, the Maastrichtian CsB7 of Fleury (1980) from Gavrovo-Tripolitza (Greece), and the upper Maastrichtian *Fleuryana adriatica* taxon-range subzone of Velić (2007) from Dinarides (Fig. 9).

Rudist are also observed in this assemblage. The rudist fauna consists mainly of radiolitids indicating a late Maastrichtian age: *Bournonia triangulata*, *B. adriatica* and *B.* cf. *quadripinnea*. These species were described together with *Rhapydionina liburnica* from the limestones of Dolenja Vas-Slovenia and Padriciano-Italy by Drobne et al. (1988), Pleničar et al. (1992) and Caffau et al. (1998).

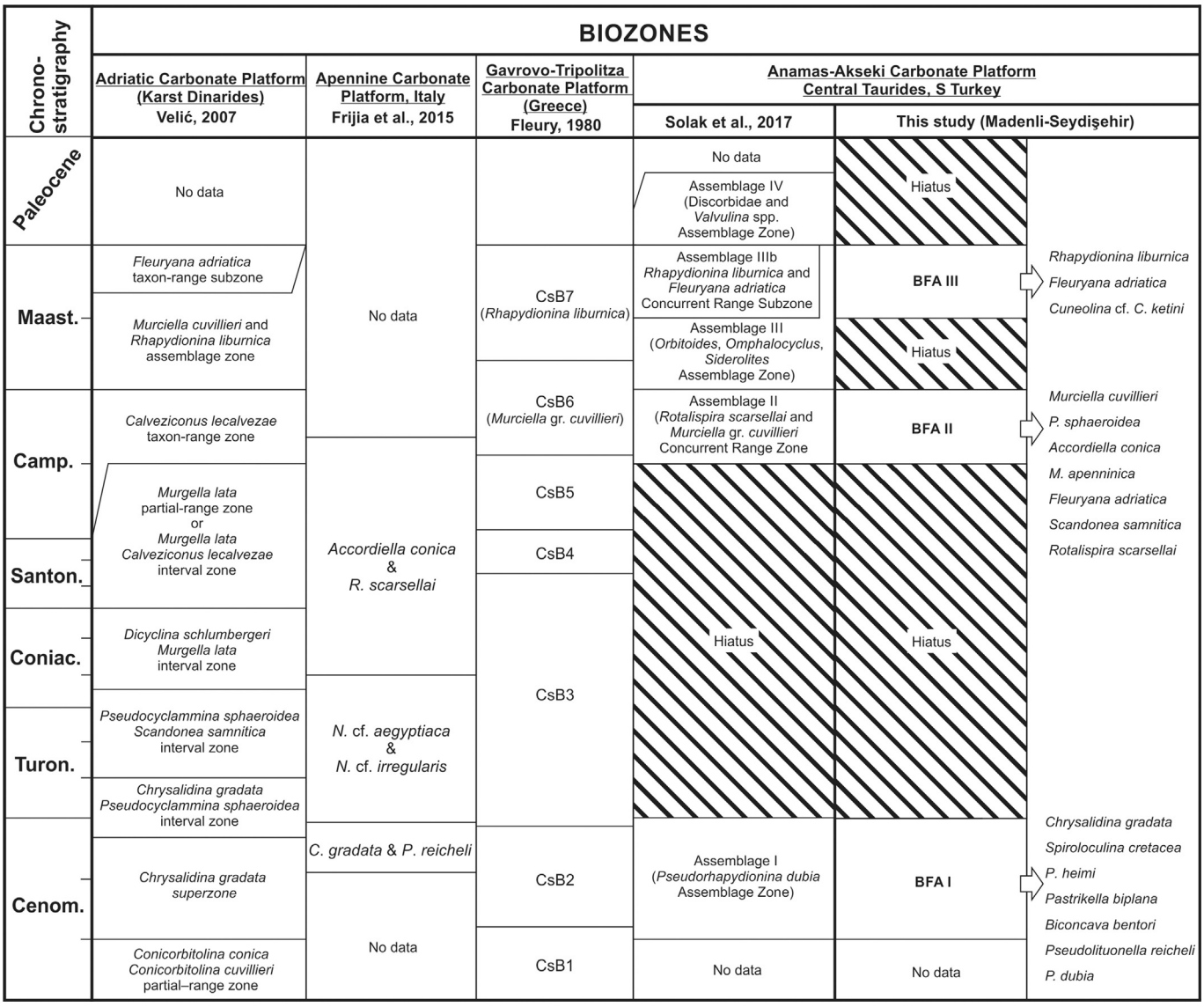

Fig. 9. Correlation of the benthic foraminiferal biozones defined in the Upper Cretaceous carbonate platforms of the Tethyan realm.

Joufia cappadociencis and *Biradiolites* sp. are also associated to this rudist fauna.

The overlying limestones contain rare *Miscellanea* sp. (Fig. 12(A, B)), Discorbidae (Fig. 12(C)), *Valvulina* aff. *V. triangularis* (Fig. 12(D–G)), Rotaliidae indet. (Fig. 12(H)), *Valvulina* sp. (Fig. 12(I–K)), abundant dasycladalean algae *Acicularia* sp. (Fig. 12(L)), *Clypeina bucuri* (Fig. 12(M–S)), and *Microcodium* sp. (Fig. 12(T)). Based on the presence of *Clypeina bucuri*, these limestones are assigned to the early Eocene (Sokač et al., 2012; Dr. Felix Schlagintweit, pers. comm. 2018).

5. Discussion

The Madenli succession represents the eastern part of the Anamas-Akseki Platform. In this area, carbonate sedimentation took place in restricted inner platform conditions during the Late Cretaceous and was frequently interrupted by emersions (Table 2), resulting in relatively thin carbonate deposits. While the Madenli succession has a thickness less than 240 m, the Cenomanian and upper Campanian-Maastrichtian Kuyucak succession located 25 km west of the Madenli area is *ca.* 400 m thick (Solak et al., 2017).

During most of the Cenomanian time, shallow subtidal to tidal flat environments prevailed in this region. From the middle to the late Cenomanian, some parts of the platform (e.g., the Dogankuzu and Mortas areas) were subaerially exposed, leading to karstification and bauxite deposition, whereas other parts (e.g., the Madenli-I and II sections) were submerged and supratidal carbonates (subunit-1a) accumulated. Shallowing upward Cenomanian successions are widespread throughout the Taurides (Farinacci and Köylüoğlu, 1982; Taslı et al., 2006; Solak et al., 2017). This event may correspond to global-scale sea level fall in the mid Cenomanian (Haq et al., 1987) which was also recorded in other carbonate platforms in the western Tethys region (Korbar et al., 2001). Shallow marine environments were later reestablished due to relative sea level rise in the late Cenomanian, and lasted until the end of the Cenomanian in many parts of the platform. This conclusion concerning the age of the bauxite deposits in the Seydişehir area fits well to G. Bignot's statement in Özlü (1978) that the bauxite deposits formed before termination of the Cenomanian.

The post-Cenomanian gap in the Madenli succession, which is very common in the Tauride Carbonate Platform(s) (Farinacci and Köylüoğlu, 1982; Solak et al., 2017), corresponds to a global carbonate platform crisis, which lasted at least a few million years

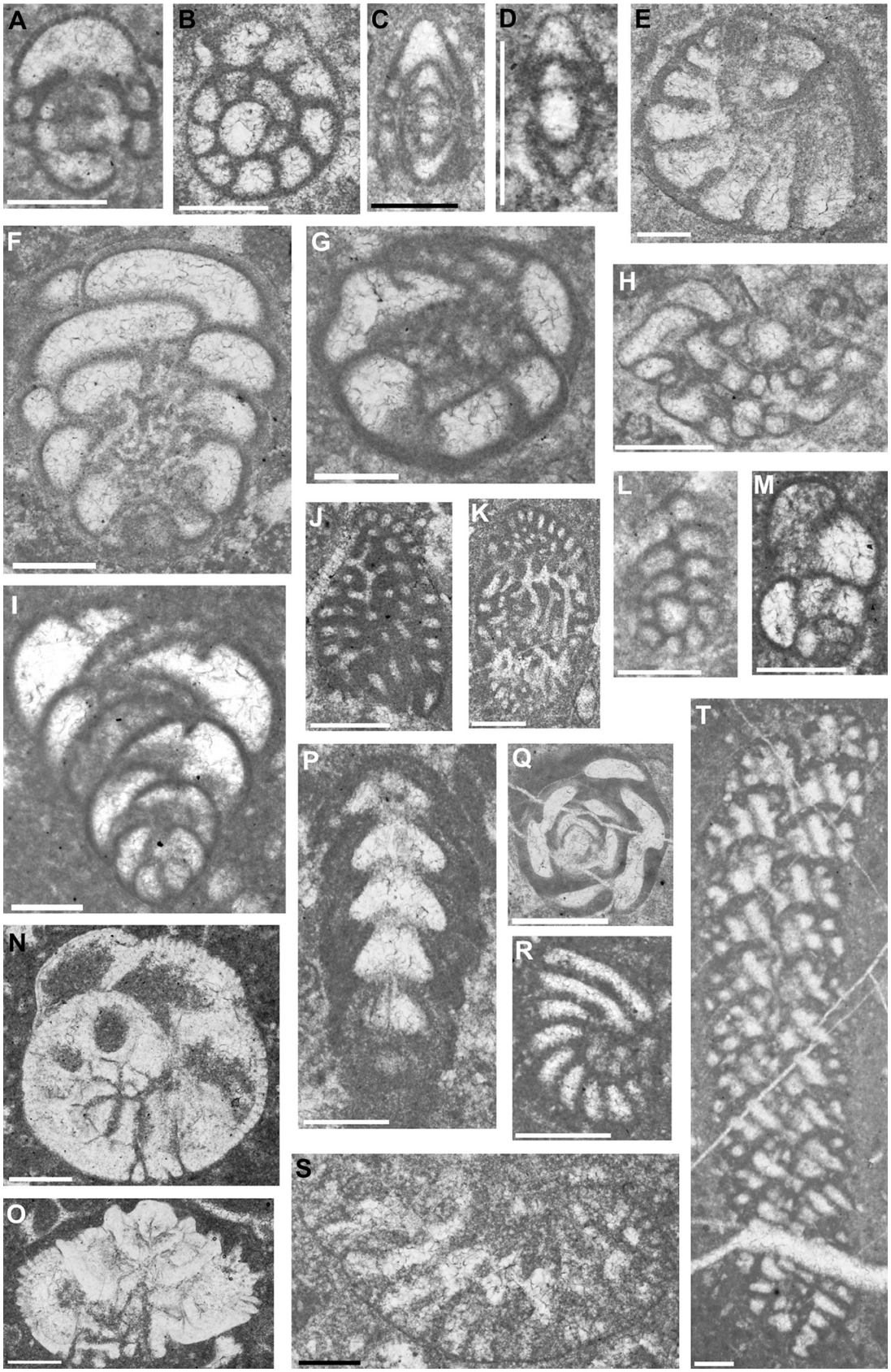

Fig. 10. Upper Campanian benthic foraminifera (BFA II). **A, B**. *Moncharmontia apenninica*, samples md116 (A), md131 (B). **C, D**. *Fleuryana adriatica*, sample md204. **E**. *Nezzazatinella* sp., sample md130. **F, G**. *Accordiella conica*, samples md205 (F), md130 (G). **H**. *Nezzazata* sp., sample md116. **I**. *Minouxia* sp., sample md123. **J, K**. *Murciella cuvillieri*, sample mda2. **L**. *Bolivinopsis* sp., sample md129. **M**. *Arenobulimina* sp., sample md205. **N, O**. *Rotalispira scarsellai*, sample mda2. **P, Q**. *Scandonea samnitica*, sample md116. **R**. *Pseudocyclammina sphaeroidea*, sample md204. **S**. *Dictyopsella kiliani*, sample md130. **T**. *Cuneolina pavonia*, sample mda2/1. Scale bars: 200 μm.

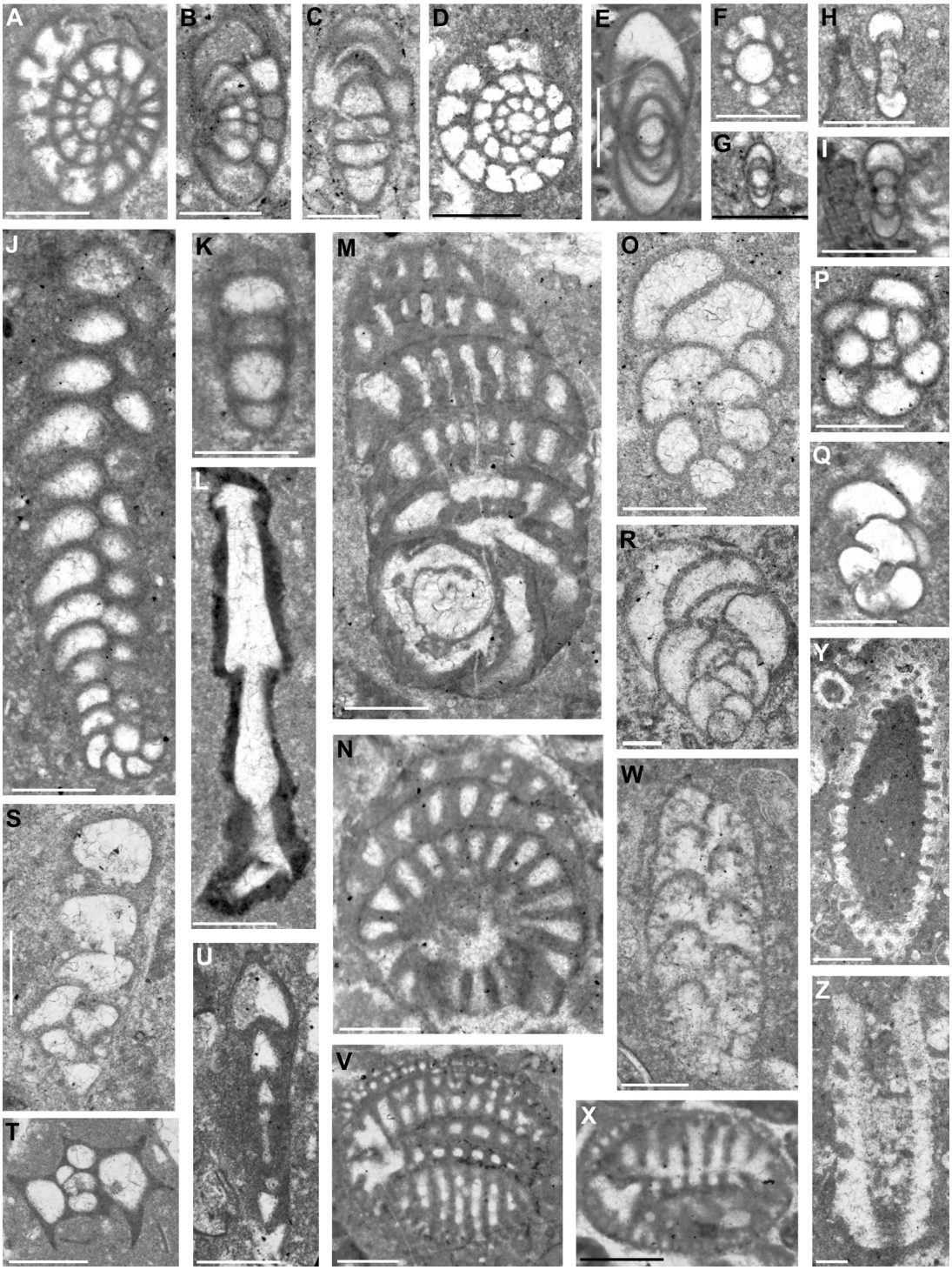

Fig. 11. Upper Maastrichtian benthic foraminifera (BFA III) and dasycladalean algae. **A–G**. *Fleuryana adriatica*, samples md41 (A), md11 (B), md14 (C), md35 (D), md61 (E), md9 (F), md11 (G). **H, I**. *Fleuryana* sp., samples md19 (H) md61 (I). **J, K**. *Bolivinopsis* sp., samples md 58 (J), md36 (K). **L**. Nubeculariidae, sample md6. **M, N**. *Rhapydionina liburnica*, samples md60 (M), md61 (N). **O–Q**. *Arenobulimina* sp., samples md5 (O), md9 (P), md9 (Q). **R**. *Minouxia* sp., sample md61. **S**. *Valvulina* aff. *V. triangularis*, sample md45. **T**. *Moesiloculina* sp., sample md37. **U**. *Elazığella* sp., sample md59. **V–X**. *Cuneolina* sp. (cf. *C. ketini*), samples md63 (V), md61 (W), md61 (X). **Y, Z**. Dasycladalean algae, sample md63. Scale bars: 200 μm.

around the Cenomanian-Turonian boundary (Schlager and Philip, 1990). But in the Anamas-Akseki Platform this platform crisis took much longer and continued up to the late Campanian. In localities where the Cenomanian bauxite deposits are directly overlain by the upper Campanian limestones (e.g., Madenli-I section in Fig. 3 and Morçukur well-log in Özlü, 1978), the bauxite deposits seem to be formed during the Turonian-early Campanian. Shallow-water platform carbonate deposition restarted during the late Campanian and then was interrupted by a third emersion period during the early Maastrichtian, which is indicated by iron-oxided surfaces, rhizolites and minor bauxite deposits (Öztürk et al., 2002). This unconformity is the cause of the lack of Unit-2 in the Doğankuzu bauxite quarry where the upper Maastrichtian unit (Unit-3) directly overlies the Cenomanian bauxite deposit (Fig. 3).

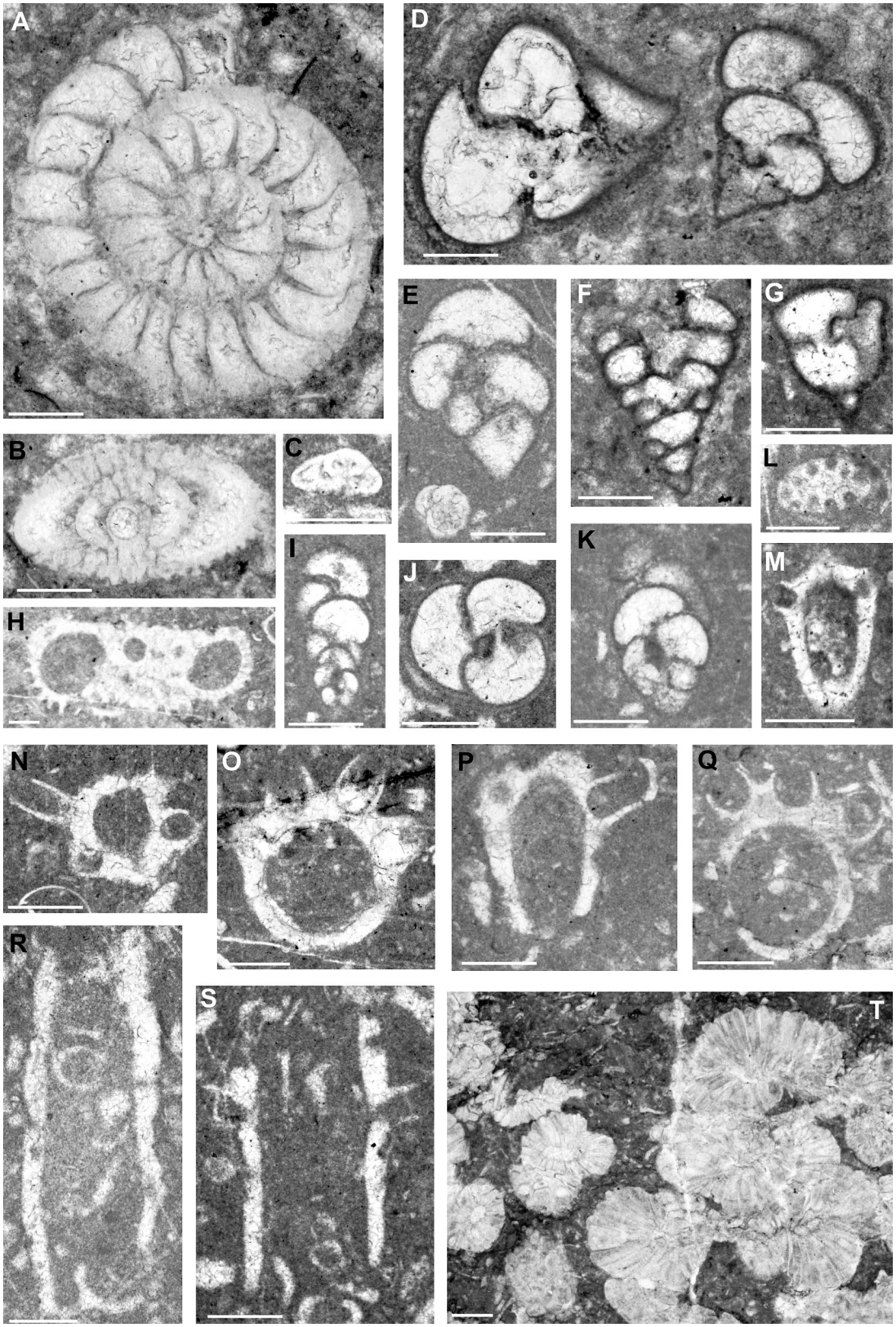

Fig. 12. Lower Eocene benthic foraminifera and dasycladalean algae. **A, B**. *Miscellanea* sp., sample md98. **C**. Discorbidae, sample md76. **D–G**. *Valvulina* aff. *V. triangularis*, samples md98 (D), md76 (E), md99 (F), md99 (G). **H**. Rotaliidae indet., sample md69. **I–K**. *Valvulina* sp., samples md100 (I), md83 (J), md99 (K). **L**. *Acicularia* sp., sample md69. **M–S**. *Clypeina bucuri*, samples md106 (M), md83 (N–P), md76 (Q–S). **T**. *Microcodium* sp., sample md84. Scale bars: 200 μm.

Table 2
Outlines of the platform evolution with biostratigraphic and sedimentological data from the Madenli Upper Cretaceous succession.

Age	Selected foraminifera	Stratigraphic and sedimentological features		Depositional environments
Lower Eocene	Limestones with Dasycladalean alga *Clypeina bucuri* and rare *Miscellanea* sp.			
Paleocene				Emerged platform
Late Maastrichtian	*Rhapydionina liburnica*, *Fleuryana adriatica*, *Cuneolina* cf. *C. ketini*	Unit-3	Laminated-dolomitic limestones and rudist-bearing limestones with carbonate breccia intercalations Benthic foraminiferal-microbial wackestone (MFA-3), bioclastic wackestone/packstone/floatstone (MFA-4), rare wackestone with *Decastronema* (MFA-5) and algal wackestone (MFA-6)	Cyclic sedimentation subtidal to intertidal/ supratidal
Early Maastrichtian				Emerged platform
Late Campanian	*Murciella cuvillieri*, *Pseudocyclammina sphaeroidea*, *Accordiella conica*, *Moncharmontia apenninica*, *Fleuryana adriatica*, *Scandonea samnitica*, *Rotalispira scarsellai*	Unit-2 upper part	Massive limestones Benthic foraminiferal-microbial wackestone (MFA-3), bioclastic wackestone/packstone/floatstone (MFA-4), rare mudstone with fenestrae/birdeyes (MFA-2)	Restricted subtidal (low energy)
Turonian to early Campanian				Emerged platform
Late Cenomanian	*Spiroloculina cretacea*, *Pseudonummoloculina heimi*, *Pseudorhapydionina dubia*, *Pseudolituonella reicheli*	Unit-2 lower part	Massive limestones Intraclastic-benthic foraminiferal packstone/grainstone, laminated peloidal packstone/grainstone (MFA-1), benthic foraminiferal-microbial wackestone (MFA-3), mudstone with fenestrae/birdeyes (MFA-2)	Dominantly shallow subtidal
Middle to late Cenomanian	*Chrysalidina gradata*, *Spiroloculina cretacea*, *Pseudonummoloculina heimi*, *Pastrikella biplana*, *Biconcava bentori*	Unit-1 upper part	Well-bedded limestones Intraclastic-benthic foraminiferal packstone/grainstone, laminated peloidal packstone/grainstone (MFA-1), sparsely mudstone with fenestrae/birdeyes, ostracod wackestone (MFA-2)	Dominantly shallow subtidal including shallow pond settings
	Bauxite deposition	Subunit 1(a)	Dolomitic-sparitic beds intercalated with bauxitic beds Laminated peloidal packstone/grainstone (MFA-1), rarely ostracod wackestone (MFA-2)	Partly Emerged platform and supratidal
	Chrysalidina gradata, *Spiroloculina cretacea*, *Pseudonummoloculina heimi*	Unit-1 lower part	Well-bedded limestones Intraclastic-benthic foraminiferal packstone/grainstone, laminated peloidal packstone/grainstone (MFA-1), sparsely mudstone with fenestrae/birdeyes, ostracod wackestone (MFA-2)	Dominantly shallow subtidal including shallow pond settings

Similarly, the Late Cretaceous gaps indicated by karst-related, unconformity-type bauxite deposits (Özlü, 1979; Öztürk et al., 2002) were recorded also on the other peri-Mediterranean carbonate platforms. In the Adriatic Carbonate Platform (AdCP), the late Cenomanian to late Santonian platform emersion is indicated by local bauxite deposits in Slovenia, Croatia and Bosnia and Herzegovina (Šparica, 1981; Dragičević and Velić, 2002; Vlahović et al., 2005). In the Central-Southern Apennines, two gaps extending from the upper Albian to the lower part of the middle Cenomanian and from the upper Cenomanian to the lower part of the Turonian or Santonian are indicated by frequently bauxitic deposits (Chiocchini et al., 1989). In the Dinarides, the uppermost Cenomanian to Santonian hiatus is marked by bauxitic deposits and the event is considered as being tectonically controlled at a regional scale, marking a forebulge stage of the Dinaridic inner-karst unit (D'Argenio and Mindszenty, 1995; Korbar, 2009).

6. Conclusions

The Madenli Upper Cretaceous succession, which represents a small part of the Tauride Carbonate Platform(s), is composed of purely platform carbonate sediments. We explained here the depositional history of this part of the platform based on new sedimentological and stratigraphical data combined with existing micropaleontological and stratigraphical information on the bauxite-bearing carbonate succession of the Seydişehir area. Benthic foraminiferal taxa, previously recorded from the peri-Mediterranean platforms, are documented and illustrated. Three biozones are identified based on the stratigraphic ranges of benthic foraminiferal taxa: BFA I in the middle to upper Cenomanian, BFA II in the upper Campanian, and BFA III in the upper Maastrichtian.

In the succession, three stratigraphic gaps are documented by means of benthic foraminiferal biostratigraphy and/or sedimentological analysis. The first one is indicated by bauxite deposits, up to 40 m thick; it corresponds to a time interval within the middle to late Cenomanian. The presence of upper Cenomanian strata overlying the bauxite deposits shows that platform carbonate deposition began again and continued until the end of the Cenomanian. The second and long-lasting, biostratigraphically evidenced one, extends from the Turonian to the early Campanian. A third one, corresponding to the early Maastrichtian, is marked by iron-oxided surfaces and rhizolites. Microfacies analysis show that deposition during the Late Cretaceous took place entirely on peritidal environments of restricted platform sensitive to eustatic sea level changes as well as local and regional tectonic movements of different platform blocks.

This study is part of ongoing works on stratigraphy and sedimentology of the Taurides Upper Cretaceous platform carbonates. A regional stratigraphic framework and paleogeographic reconstruction for the Late Cretaceous will be produced after the data from the other parts of the Taurides were completed and correlated with those of other peri-Mediterranean platforms.

Acknowledgements

This study was supported by the Scientific and Technological Research Council of Turkey (TUBITAK) with Project Number 115Y130. We thank Dr. Felix Schlagintweit for determination of

the lower Eocene Dasycladalean algae, and Samet Salar (Mersin University) for the preparation of thin sections. We thank Dr. Gilles Escarguel, Dr. Fabienne Giraud, Dr. Esmeralda Caus and two anonymous reviewers for their careful reviews and suggestions, which improved the manuscript.

Appendix A. List (in alphabetical order) of all the species mentioned in the text with their authorship

Benthic foraminifera

Accordiella conica Farinacci, 1962
Biconcava bentori Hamaoui et Saint–Marc, 1970
Chrysalidina gradata D'Orbigny, 1839
Cuneolina ketini İnan, 1988
Cuneolina pavonia D'Orbigny, 1846
Dictyopsella kiliani Munier–Chalmas, 1900
Fleuryana adriatica De Castro, Drobne et Gušić, 1994
Moncharmontia apenninica (De Castro, 1968)
Murciella cuvillieri Fourcade, 1966
Murgeina apula (Luperto Sinni, 1968)
Nezzazata gyra (Smout, 1956)
Nezzazata simplex Omara, 1956
Nezzazatinella picardi (Henson, 1948)
Nummoloculina regularis Philippson, 1887
Pastrikella biplana Cherchi et Schroeder, 1980
Pseudocyclammina sphaeroidea Gendrot, 1968
Pseudolituonella reicheli Marie, 1954
Pseudonummoloculina heimi (Bonet, 1956)
Pseudorhapydionina dubia (De Castro, 1965)
Rhapydionina liburnica Stache, 1913
Rotalispira scarsellai (Torre, 1966)
Scandonea samnitica De Castro, 1971
Spiroloculina cretacea Reuss, 1854
Valvulina triangularis D'Orbigny, 1826

Rudists

Bournonia adriatica Pejović, 1970
Bournonia quadripinnea Pejović, 1988
Bournonia triangulata Pleničar et Zucchi–Stolfa, 1988
Joufia cappadociencis (Cox, 1960) Karacabey, 1969

Others

Decastronema barattoloi (De Castro, 1989)
Decastronema kotori (Radoičić, 1959)

References

Aguilera-Franco, N., 2003. Cenomanian-Coniacian zonation (foraminifers and calcareous algae) in the Guerrero-Morelos basin, southern Mexico. Revista Mexicana de Ciencias Geológicas 20, 202–222.

Andrew, T., Robertson, A.H.F., 2002. The Beyşehir-Hoyran-Hadım Nappes: Mesozoic marginal and oceanic units of the Northern Neotethys in Southern Turkey. Journal of the Geological Society, London 159, 529–543.

Atabey, M.E., 1976. Mortaş boksit yatağının mineralojisi, kimyası ve kökeni.(Mineralogy, chemistry and origin of the Mortaş bauxite deposit). Bulletin of the Geological Society of Turkey 19, 9–14.

Blumenthal, M., Göksu, E., 1949. Die bauxitvorkommen der Berge um Akseki Erörterungen über ihre geologische position, ausmasse und genese. Mineral Research and Exploration Institute (MTA) 14, 59.

Caffau, M., Pleničar, M., Pugliese, N., Drobne, K., 1998. Late Maastrichtian rudists and microfossils in the Karst Region (NE Italy and Slovenia). Geobios Mémoire Spécial 22, 37–46.

Carannante, G., Ruberti, D., Sirna, G., 1998. Senonian rudist limestones in the Sorrento Peninsula sequences (Southern Italy). Geobios Mémoire Spécial 22, 47–68.

Carannante, G., Ruberti, D., Sirna, M., 2000. Upper Cretaceous ramp limestones from the Sorrento Peninsula (southern Apennines, Italy): micro- and macrofossil associations and their significance in the depositional sequences. Sedimentary Geology 132, 89–123.

Chiocchini, M., 2008. The new genus *Palaeocornuloculina* (Foraminiferida, Cornuspiracea) and its species from Cenomanian limestones of Southern Latium (Central Italy). Memorie Descrittive della Carta Geologica d'Italia 84, pp. 203–224.

Chiocchini, M., Mancinelli, A., Romano, A., 1989. The gaps in the Middle-Upper Cretaceous carbonate series of the southern Apennines (Abruzzi and Campania regions). Geobios Mémoire Spécial 11, 133–149.

Chiocchini, M., Mancinelli, A., 2001. *Sivasella monolateralis* Sirel and Gunduz, 1978 (Foraminiferida) in the Maastrichtian of Latium (Italy). Revue de Micropaléontologie 44, 267–277.

Chiocchini, M., Chiocchini, R.A., Didaskalou, P., Potetti, M., 2008. Microbiostratigrafia del Triassico superiore, Giurassico e Cretacico in facies di piattaforma carbonatica del Lazio centro-meridionale e Abruzzo: revisione finale. In: Chiocchini, M. (Ed.). Memorie Descrittive della Carta Geologica d'Italia, Torino, 84, pp. 5–170.

Chiocchini, M., Pichezz, R.M., 2016. *Cairoella tricamerata* n. gen., n. sp. (Foraminiferida, Milioloidea) from the lower Cenomanian of Monte Cairo (Southern Latium, Central Italy). Rivista Italiana di Paleontologia e Stratigrafia 122, 77–84.

D'argenio, B., Mindszenty, A., 1995. Bauxites and related paleokarst: tectonic and climatic event markers at regional unconformities. Eclogae Geologicae Helvetiae 88, 453–499.

Dean, W.T., Monod, O., 1970. The Lower Palaeozoic stratigraphy and faunas of the Taurus Mountains near Beyşehir, Turkey. I. Stratigraphy. Bulletin of the British Museum of Natural History, Geology 19, 413–426.

Demirtaşlı, E., 1984. Stratigraphy and tectonics of the area between Silifke and Anamur, Central Taurus Mountains. In: Tekeli, O., Göncüoğlu, M.C. (Eds.), Geology of the Taurus Belt. Proceedings. Mineral Research and Exploration Institute-Geological Society of Turkey, Ankara, pp. 101–118.

Dragičević, I., Velić, I., 2002. The northeastern margin of the Adriatic Carbonate Platform. Geologia Croatica 55, 185–232.

Drobne, K., Ogerelec, B., Pleničar, M., Zucchi Stolfa, M.L., Turnk, D., 1988. Maastrichtian, Danian, and Thanetian beds in Dolenja Vas (NW Dinarides, Yugoslavia) microfacies, foraminifers, rudist and corals. Razprave 29, 147–224.

Dumont, J.F., 1976. La courbure d'Isparta et l'origine des nappes d'Antalya ; hypothèse d'un décrochement majeur, l'accident trans-taurique, qui a dédoublé le dispositif structural taurique établi par la tectogenèse du Crétacé superieur. Bulletin of Mineral Resources Exploration of Turkey 86, 56–67.

Dumont, J.F., Kerey, E., 1975. Eğridir gölü güneyinin temel jeolojik etüdü.(Basic geological study of southern lake of Eğridir). Bulletin of the Geological Society of Turkey 18, 169–174 (in Turkish).

Dunham, R.J., 1962. Classification of carbonate rocks according to depositional texture. In: Ham, W.E. (Ed.), Classification of carbonate rocks. American Association of Petroleum Geologists Memoir, Tulsa, pp. 108–121.

Embry, A.F., Klovan, J.E., 1971. A Late Devonian reef tract on northeastern Banks Island. Northwest Territories. Canadian Petroleum Geology Bulletin 33, 730–781.

Farinacci, A., Köylüoğlu, M., 1982. Evolution of the Jurassic-Cretaceous Taurus shelf (Southern Turkey). Estratto dal Bollettino della società Paleontologica Italiana 21, 267–276.

Fleury, J.-J., 1980. Les zones de Gavrovo-Tripolitza et du Pinde-Olonos (Grèce continentale et Péloponnèse du Nord) : évolution d'une plate-forme et d'un bassin dans leur cadre alpin. Société Géologique du Nord 4, 1–651.

Fleury, J.-J., 2014. Données nouvelles sur *Rhapydionina* Stache, 1913 et *Fanrhapydionina* n. gen., un groupe de Rhapydioninidae (Alveolinacea, Foraminifera) foisonnant en région périadriatique au Campanien-Maastrichtien. Geodiversitas 36, 173–208.

Fleury, J.-J., 2016. *Cuvillierinella salentina* (Foraminifera, Rhapydioninidae) and its kindship in the Western Mediterranean area during the Campanian-Maastrichtian. Revue de micropaléontologie 59, 200–224.

Flügel, E., 2004. Microfacies of carbonate rocks: analysis, interpretation and application. Springer-Verlag, Berlin Heidelberg976.

Frijia, G., Parente, M., Di Lucia, M., Mutti, M., 2015. Carbon and strontium isotope stratigraphy of the Upper Cretaceous (Cenomanian-Campanian) shallow-water carbonates of southern Italy: chronostratigraphic calibration of larger foraminifera biostratigraphy. Cretaceous Research 53, 110–139.

Golubic, S., Radoičić, R., Seong-Joo, L., 2006. *Decastronema kotori* gen. nov., comb. nov.; a mat-forming cyanobacterium on Cretaceous carbonate platforms and its modern counterparts. Carnets de Géologie 127 (2) Article 2006/2.

Gradstein, F.M., Ogg, J.G., Hilgen, F.J., 2012. On The Geologic Time Scale. Newsletters on Stratigraphy 45, 171–188.

Haq, B.U., Hardenbol, J., Vail, P.R., 1987. Chronology of fluctuating sea levels since the Triassic. Science 235, 1156–1167.

Karadağ, M.M., Küpeli, Ş., Arık, F., Ayhan, A., Zedef, V., Döyen, A., 2009. Rare earth element (REE) geochemistry and genetic implications of the Mortaş bauxite deposit (Seydişehir/Konya-Southern Turkey). Chemie der Erde 69, 143–159.

Korbar, T., 2009. Orogenic evolution of the External Dinarides in the NE Adriatic region: a model constrained by tectonostratigraphy of Upper Cretaceous to Paleogene carbonates. Earth Science Reviews 96, 296–312.

Korbar, T., Fuček, L., Husinec, A., Vlahović, I., Oštrić, N., Matičec, D., Jelaska, V., 2001. Cenomanian Carbonate Facies and Rudists along shallow intraplatform basin margin-the Island of Cres (Adriatic Sea, Croatia). Facies 45, 39–58.

Martin, C., 1969. Akseki kuzeyindeki bir kısım Toroslar'ın stratigrafik ve tektonic incelemesi.(Stratigraphic and tectonic investigation of a part of the Taurides in North of Akseki). Bulletin of Mineral Resources Exploration of Turkey 72, 110–129 (in Turkish).

Monod, O., 1977. Recherches géologiques dans le Taurus occidental au sud de Beyşehir (Turquie) Ph.D. Thesis. Université de Paris-Sud Orsay (unpubl.).

Özgül, N., 1976. Torosların bazı temel jeolojik özellikleri. Geological Society of Turkey Bulletin 19, 65–78.

Özgül, N., 1984. Stratigraphy and tectonic evolution of the Central Taurides. In: Tekeli, O., Göncüuğlu, M.C. (Eds.), Geology of the Taurus Belt. Proceedings. Mineral Research and Exploration Institute-Geological Society of Turkey, Ankara, pp. 77–90.

Özgül, N., 1978. Étude géologique, minéralogique et géochimique des bauxites de la région D'Akseki-Seydişehir (Taurus Occidental-Turquie) Ph.D. Thesis. Université Pierre-et-Marie-Curie (unpubl.).

Özlü, N., 1979. Akseki-Seydişehir Boksitlerinin Kökeni Hakkında Yeni Bulgular.(-New facts on the genesis of the Akseki-Seydişehir bauxite deposits). Bulletin of the Geological Society of Turkey 22, 215–226.

Öztürk, H., Hein, J.R., Hanılçı, N., 2002. Genesis of the Doğankuzu and Mortaş Bauxite deposits, Taurides, Turkey: separation of Al, Fe, and Mn and implications for passive margin Metallogen. Economic Geology 97, 1053–1077.

Pleničar, M., Drobne, K., Ogorelec, B., 1992. Rudists and larger foraminifera below the Cretaceous-Tertiary boundary in the Dolenja vas section. In: Kolmann, H.A., Zapfe, H. (Eds.). New aspects on Tethyan Cretaceous fossil assemblages. Österreichische Akademie der Wissenschaften, Schriftenreihe der erdwissenschaftlichen Kommissionen 9, pp. 231–240.

Poisson, A., Akay, E., Dumont, J.F., Uysal, Ş., 1984. The Isparta angle: a Mesozoic paleorift in the Western Taurides. In: Tekeli, O., Göncüoğlu, M.C. (Eds.). In: Proceedings of the International Symposium on the Geology of the Taurus Belt 1983, Ankara, pp. 11–26.

Ruberti, D., 1997. Facies analysis of a Upper Cretaceous highenergy rudist-dominated carbonate ramp (Matese Mts., central-southern Apennines, Italy): subtidal and peritidal cycles. Sedimentary Geology 103, 81–110.

Sarı, B., Taslı, K., Özer, S., 2009. Benthonic foraminiferal biostratigraphy of the Upper Cretaceous (middle Cenomanian-Coniacian) sequences of the Bey Dağları carbonate platform, Western Taurides, Turkey. Turkish Journal of Earth Sciences 18, 393–425.

Schlager, W., Philip, J., 1990. Cretaceous carbonate platforms. In: Ginsburg, N., Beaudoin, B. (Eds.), Cretaceous Resources, Events and Rhythms, 304, Kluwer, Dordrecht, pp. 173–195.

Solak, C., Taslı, K., Koç, H., 2017. Biostratigraphy and facies analysis of the Upper Cretaceous-Danian? platform carbonate succession in the Kuyucak area, western Central Taurides, S Turkey. Cretaceous Research 79, 43–63.

Šparica, M., 1981. Mezozoik Banije, Korduna i dodirnog područja Bosne.(Geology of the Mesozoic areas of Kordun, Banija and NW Bosnia, Yugoslavia). Nafta Spec. Mem. 12, 245.

Sokač, B., Velić, I., Grgasović, T., Ćosović, V., Vlahović, I., 2012. Taxonomy and stratigraphy of an algal assemblage in Palaeogene deposits of the northern foothills of Mt. Biokovo (Southern Croatia). Geologia Croatica 65, 161–205.

Steuber, T., Korbar, T., Jelaska, V., Gušić, I., 2005. Strontium isotope stratigraphy of Upper Cretaceous platform carbonates of the island of Brač (Adriatic Sea, Croatia): implications for global correlation of platform evolution and biostratigraphy. Cretaceous Research 26, 741–756.

Taslı, K., Özer, E., Koç, H., 2006. Benthic foraminiferal assemblages of the Cretaceous platform carbonate succession in the Yavca area (Bolkar Mountains, S Turkey): biostratigraphy and paleoenvironments. Geobios 39, 521–533.

Velić, I., 2007. Stratigraphy and palaeobiogeography of Mesozoic benthic foraminifera of the Karst Dinarides (SE Europe). Geologica Croatica 60, 1–113.

Velić, I., Vlahović, I., 1994. Foraminiferal assemblages in the Cenomanian of the Buzet-Savudrija area (Northwestern Istria, Croatia). Geologia Croatia 47, 25–43.

Vlahović, I., Tišljar, J., Velić, I., Matičec, D., 2005. Evolution of the Adriatic Carbonate Platform: palaeogeography, main events and depositional dynamics. Palaeogeography, Palaeoclimatology, Palaeoecology 220, 333–360.

Wippern, J., 1962. Toros boksitleri ve bunların tektonik durumu.(Taurus bauxites and their tectonic state). Bulletin of Mineral Resources Exploration of Turkey 58, 47–70 (in Turkish).